CHAPTER 18

INTERNAL DOSIMETRY

C. HINDORF
Department of Radiation Physics,
Skåne University Hospital,
Lund, Sweden

18.1. THE MEDICAL INTERNAL RADIATION DOSE FORMALISM

18.1.1. Basic concepts

The Committee on Medical Internal Radiation Dose (MIRD) is a committee within the Society of Nuclear Medicine. The MIRD Committee was formed in 1965 with the mission to standardize internal dosimetry calculations, improve the published emission data for radionuclides and enhance the data on pharmacokinetics for radiopharmaceuticals [18.1]. A unified approach to internal dosimetry was published by the MIRD Committee in 1968, MIRD Pamphlet No. 1 [18.2], which was updated several times thereafter. Currently, the most well known version is the MIRD Primer from 1991 [18.3]. The latest publication on the formalism was published in 2009 in MIRD Pamphlet No. 21 [18.4], which provides a notation meant to bridge the differences in the formalism used by the MIRD Committee and the International Commission on Radiological Protection (ICRP) [18.5]. The formalism presented in MIRD Pamphlet No. 21 [18.4] will be used here, although some references to the quantities and parameters used in the MIRD Primer [18.3] will be made. All symbols, quantities and units are presented in Tables 18.1 and 18.2.

The MIRD formalism gives a framework for the calculation of the absorbed dose to a certain region, called the target region, from activity in a source region. The absorbed dose D is calculated as the product between the time-integrated activity $\tilde{A}$ and the S value:

$$D = \tilde{A} \cdot S \tag{18.1}$$

The International System of Units unit of absorbed dose is the joule per kilogram (J/kg), with the special name gray (Gy) (1 J/kg = 1 Gy).

The time-integrated activity equals the number of decays that take place in a certain source region, with units Bq · s, while the *S* value denotes the absorbed dose rate per unit activity, expressed in Gy · (Bq · s)$^{-1}$ or as a multiple thereof, for example, in mGy · (MBq · s)$^{-1}$. The time-integrated activity was named the cumulated activity in the MIRD Primer [18.3] and the absorbed dose rate per unit activity was named the absorbed dose per cumulated activity (or the absorbed dose per decay). A source or a target region can be any well defined volume, for example, the whole body, an organ/tissue, a voxel, a cell or a subcellular structure. The source region is denoted r_S and the target region r_T:

$$D(r_T) = \tilde{A}(r_S) \cdot S(r_T \leftarrow r_S) \tag{18.2}$$

The number of decays in the source region, denoted the time-integrated activity, is calculated as the area under the curve that describes the activity as a function of time in the source region after the administration of the radiopharmaceutical ($A(r_S, t)$). The activity in a region as a function of time is commonly determined from consecutive quantitative imaging sessions, but it could also be assessed via direct measurements of the activity on a tissue biopsy, a blood sample or via single probe measurements of the activity in the whole body. Compartmental modelling is a theoretical method that can be used to predict the activity in a source region in which measurements are impossible.

$$\tilde{A}(r_S) = \int A(r_S,t)\, \mathrm{d}t \tag{18.3}$$

The time-integration period T_D, for which the time-integrated activity in the source region is determined, is commonly chosen from the time of administration of the radiopharmaceutical until infinite time, e.g. 0 to ∞ (Eq. (18.4)). However, the integration period should be matched to the biological end point studied in combination with the time period in which the relevant absorbed dose is delivered.

$$\tilde{A}(r_S,T_D) = \int_0^{T_D} A(r_S,t)\, \mathrm{d}t \tag{18.4}$$

The time-integrated activity coefficient $\tilde{a}$ is defined as the time-integrated activity divided by the administered activity A_0, as can be seen in Eq. (18.5), and has the unit of time. The time-integrated activity coefficient was named the 'residence time' in the MIRD Primer [18.3]. Figure 18.1 further demonstrates the

concept. The area under the curve describing the activity as a function of time equals the area for the rectangle ($\int_0^{T_D} A(r_S,t)\ \mathrm{d}t = \tilde{a}(r_S)\cdot A_0$) and the time-integrated activity coefficient can be described as an average time that the activity spends in a source region.

$$\tilde{a}(r_S) = \frac{\tilde{A}(r_S)}{A_0} \tag{18.5}$$

The S value is defined according to Eq. (18.6), which includes the energy emitted E, the probability Y for radiation with energy E to be emitted, the absorbed fraction ϕ and the mass of the target region $M(r_T)$. The absorbed fraction is defined as the fraction of the energy emitted from the source region that is absorbed in the target region and equals a value between 0 and 1. The absorbed fraction is dependent on the shape, size and mass of the source and target regions, the distance and type of material between the source and the target regions, the type of radiation emitted from the source and the energy of the radiation:

$$S = \frac{EY\phi}{M(r_T)} \tag{18.6}$$

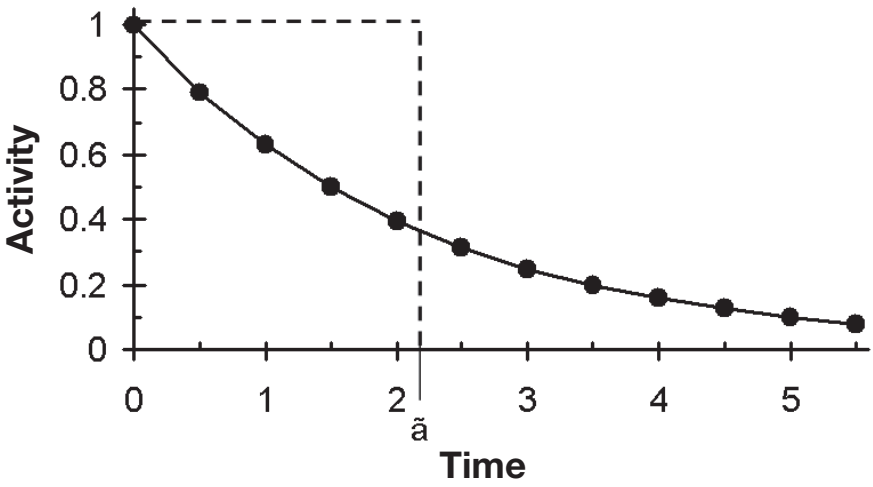

FIG. 18.1. The time-integrated activity coefficient (the residence time in the MIRD Primer [18.3]) is calculated as the time-integrated activity divided by the injected activity, which gives an average time the activity spends in the source region.

The product of the energy emitted E and its probability to be emitted Y is denoted Δ, the mean energy emitted per decay of the radionuclide. The full formalism also includes a summation over all of the transitions i per decay:

$$S(r_T \leftarrow r_S) = \sum_i \frac{\Delta_i \phi(r_T \leftarrow r_S, i)}{M(r_T)} \tag{18.7}$$

The absorbed fraction divided by the mass of the target region is named the specific absorbed fraction Φ:

$$\Phi(r_T \leftarrow r_S, E_i) = \frac{\phi(r_T \leftarrow r_S, E_i)}{M(r_T)} \tag{18.8}$$

The mass of both the source and target regions can vary in time, which means that the absorbed fraction will change as a function of time after the administration, and the full time dependent version of the internal dosimetry nomenclature must be applied (Eq. (18.9)). This phenomenon has been noted in the clinic for tumours, the thyroid and lymph nodes, and can significantly influence the magnitude of the absorbed dose.

$$\Phi(r_T \leftarrow r_S, E_i, t) = \frac{\phi(r_T \leftarrow r_S, E_i, t)}{M(r_T, t)} \tag{18.9}$$

The total mean absorbed dose to the target region $D(r_T)$ is given by summing the separate contributions from each source region r_S (Eq. (18.10)). The self-absorbed dose commonly gives the largest fractional contribution to the total absorbed dose in a target region. The self-absorbed dose refers to when the source and target regions are identical, while the cross-absorbed dose refers to the case in which the source and the target regions are different from each other.

$$D(r_T) = \sum_{r_S} \tilde{A}(r_S) S(r_T \leftarrow r_S) \tag{18.10}$$

The full time dependent version of the MIRD formalism can be found in Eq. (18.11), where $\dot{D}$ denotes the absorbed dose rate:

$$D(r_T, T_D) = \sum_{r_S} \int_0^{T_D} \dot{D}(r_T, t)\, \mathrm{d}t = \sum_{r_S} \int_0^{T_D} A(r_S, t) S(r_T \leftarrow r_S, t)\, \mathrm{d}t \tag{18.11}$$

TABLE 18.1. EXPLANATION OF SYMBOLS USED IN THE MEDICAL INTERNAL RADIATION DOSE FORMALISM

Symbol	Parameter
R	Type of radiation
r_S	Source region
r_T	Target region
T_D	Integration period

TABLE 18.2. EXPLANATION OF THE SYMBOLS USED TO REPRESENT QUANTITIES IN THE MEDICAL INTERNAL RADIATION DOSE FORMALISM

Symbol	Quantity	Unit
$\tilde{A}(r_S,T_D)$	Time-integrated activity	Bq · s
$\tilde{a}(r_S,T_D)$	Time-integrated activity coefficient	s
$D(r_T)$	Absorbed dose to the target region r_T	Gy
$\dot{D}$	Absorbed dose rate	Gy/s
Δ_i	Mean energy of the ith transition per nuclear transformation	J (Bq · s)$^{-1}$ or MeV (Bq · s)$^{-1}$
E_i	Mean energy of the ith transition	J or MeV
$M(r_T, t)$	Mass of target region	kg
$S(r_T \leftarrow r_S,t)$	Absorbed dose rate per unit activity	mGy (MBq · s)$^{-1}$
t	Time	s
Y_i	Number of ith transitions per nuclear transformation	(Bq · s)$^{-1}$
$\phi(r_T \leftarrow r_S,E_i,t)$	Absorbed fraction	Dimensionless
$\Phi(r_T \leftarrow r_S,E_i,t)$	Specific absorbed fraction	kg^{-1}

18.1.2. The time-integrated activity in the source region

The physical meaning of the time-integrated activity in the source region would be the number of decays in the source region during the relevant time period. The time-integrated activity was named the cumulated activity in the MIRD Primer [18.3].

The activity as a function of time $A(t)$ can often be described by a sum of exponential functions (Eq. (18.12)), where j denotes the number of exponentials, A_j the initial activity for the jth exponential, λ the decay constant for the radionuclide, λ_j the biological decay constant and t the time after the administration of the radiopharmaceutical. The sum of the j coefficients A_j gives the total activity in the source region at the time of administration of the radiopharmaceutical ($t = 0$):

$$A(r_T,t) = \sum_j A_j \cdot e^{-t(\lambda+\lambda_j)} \tag{18.12}$$

The decay constant λ equals the natural logarithm of 2 (ln 2 = 0.693) divided by the half-life. The decay constant in an exponential function matches the slope of the curve it describes (in a linear-log plot of the function).

$$\lambda = \frac{\ln 2}{T_{1/2}} \tag{18.13}$$

The physical half-life $T_{1/2}$ and the biological half-life $T_{1/2,j}$ can be combined into an effective half-life $T_{1/2,\text{eff}}$ according to Eq. (18.14). The effective half-life is always shorter than both the biological and the physical half-lives alone.

$$\frac{1}{T_{1/2,\text{eff}}} = \frac{1}{T_{1/2,j}} + \frac{1}{T_{1/2}} \tag{18.14}$$

The cumulated activity for the relevant time period is commonly calculated as the time integral of an exponential function (Eq. (18.15)). However, other functions could be used, with trapezoidal or Riemann integration (Fig. 18.2). The trapezoidal and the Riemann methods could be reproduced with a higher accuracy than the integration of an exponential, depending on how well the exponential fit could be performed.

$$\tilde{A} = \int_0^\infty A(r_S,0)\, e^{-t(\lambda+\lambda_j)}\, dt = \frac{A(r_S,0)}{\lambda+\lambda_j} \tag{18.15}$$

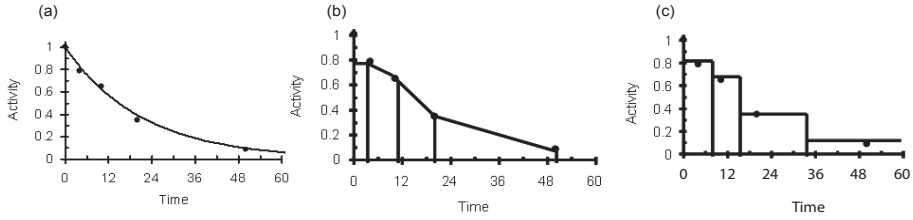

FIG. 18.2. Demonstration of different methods to calculate the time-integrated activity using a fit to an exponential function (a), trapezoidal integration (b) and Riemann integration (c).

Relevant biological data need to be acquired to perform absorbed dose calculations with accuracy. The shape of the fitted curve, which describes the activity as a function of time after the administration of the radiopharmaceutical, can be strongly influenced by the number and timing of the individual activity measurements (see Fig. 18.3). Three data points per exponential phase should be considered the minimum data required to determine the pharmacokinetics, and data points should be followed for at least two to three effective half-lives.

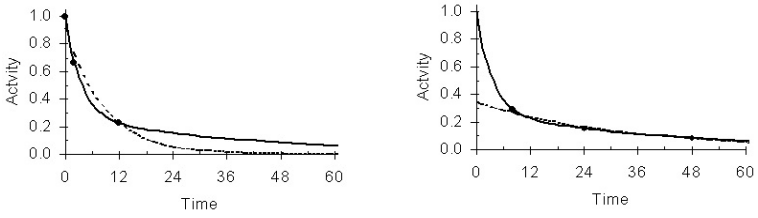

FIG. 18.3. Two examples of the possible influences of curve fitting caused by the number and the timing of activity measurements. The solid line gives the real activity versus time; the dotted line represents the exponential curve fitted to the measurements, which are shown as black dots.

The extrapolation from time zero to the first measurement of the activity in the source region, and the extrapolation from the last measurement of the activity in the source region to infinity, can also strongly influence the accuracy in the time-integrated activity (see Fig. 18.4).

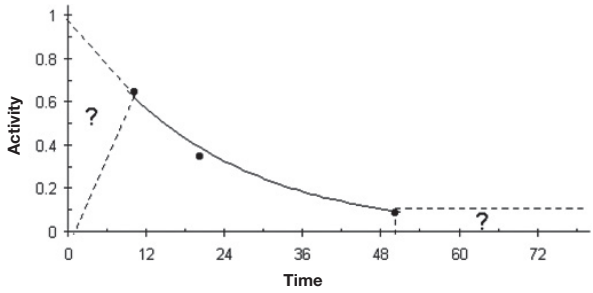

FIG. 18.4. Extrapolation before the first and after the last measurement point.

18.1.3. Absorbed dose rate per unit activity (*S* value)

The *S* value for a certain radionuclide and source–target combination is generated from Monte Carlo simulations in a computer model of the anatomy.

The first models were analytical phantoms, in which the anatomy was described by analytical equations. A coordinate system was introduced and simple geometrical shapes such as spheres or cylinders were placed in the coordinate system to represent important structures of the anatomy. Several analytical phantoms exist: adult man, non-pregnant woman, pregnant woman for each trimester of pregnancy, children (from the newborn and up to 15 years of age) as well as models of the brain, kidneys and unit density spheres.

Voxel based phantoms are the second generation of phantoms used for the calculation of *S* values. These phantoms offer the possibility of more detailed models of the anatomy. Voxel based phantoms can be based on the segmentation of organs from tomographic image data, such as computed tomography (CT) images.

The third generation of phantoms is created using non-uniform rational B-spline (NURBS). NURBS is a mathematical model used in computer graphics to represent surfaces. NURBS provides a method to represent both geometrical shapes and free forms with the same mathematical representation, and the surfaces are flexible and can easily be rotated and translated. This means that movements in time, such as breathing and the cardiac cycle, can be included, allowing for 4-D representations of the phantoms [18.6].

Anatomical phantoms for the calculation of *S* values for use in pre-clinical studies on dogs, rats and mice have also been developed.

A common assumption in radionuclide dosimetry is that radiation emissions can be divided into penetrating (p) or non-penetrating (np) and that the absorbed fractions for these two types can be set to equal 0 and 1, respectively ($\phi_p \approx 0$ and $\phi_{np} \approx 1$). Electrons are often considered non-penetrating and photons

as penetrating radiation, but this is an oversimplification. The validity of the assumption is very dependent on the energy of the radiation in combination with the size of the source region and must, therefore, be assessed on a case by case basis, as is evident from Fig. 18.5. For electrons, the absorbed fraction is greater than 0.9 if the mass of the unit density sphere is greater than 10 g and the electron energy is lower than 1 MeV. This means that the approximation of electrons as non-penetrating radiation is good at an organ level for humans, but as the mass decreases, the approximation ceases to be valid. For photons, the absorbed fraction is less than 0.1 if the mass of the sphere is less than 100 g and if the photon energy is larger than 50 keV. The approximation of considering photons as penetrating radiation is valid in most pre-clinical situations, but as the mass increases, the approximation becomes inappropriate.

The self absorbed S values can be scaled by mass according to the following equation:

$$S(r_T \leftarrow r_T, \text{scaled}) \approx S(r_T \leftarrow r_T, \text{tabulated}) \cdot \frac{M(r_T, \text{tabulated})}{M(r_T, \text{scaled})} \tag{18.16}$$

This is a useful method to adjust the S value found in a table to the true weight of the target region. When scaling an S value, the absorbed fraction is considered to be constant in the interval of scaling. The change in the S value is then set equal to the change in mass of the target. It should be noted that linear interpolation should never be performed in S value tables (Fig. 18.6).

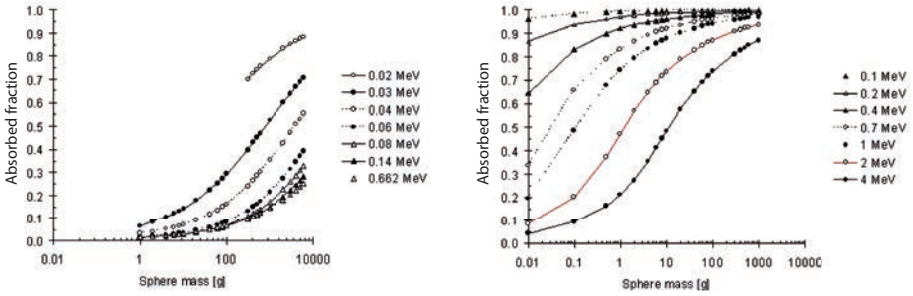

FIG. 18.5. Absorbed fraction for unit density spheres as a function of the mass of the spheres for mono-energetic photons (left) and electrons (right) (data from Ref. [18.7]).

A more sophisticated and probably more accurate way of recalculation of the S value is by separating the total S value into two parts: one for penetrating and one for non-penetrating radiation (S_p and S_{np}, respectively). If the absorbed fraction for non-penetrating radiation is assumed to be equal to 1 ($\phi_{np} = 1$), the S value for penetrating radiation can be calculated (Eqs (18.17)–(18.19)).

The absorbed fractions for photons are relatively constant, so the *S* value for penetrating radiation can be scaled by mass.

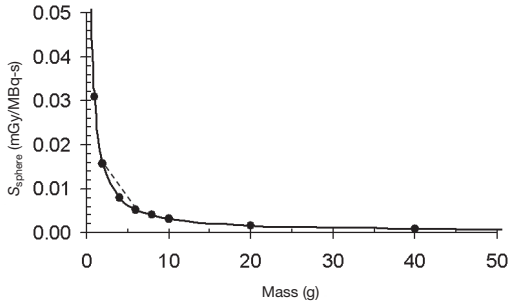

FIG. 18.6. Linear interpolation in S value tables gives S values that are too large. In this particular case for a unit density sphere of ^{131}I, linear scaling would give an S value that is significantly greater than when scaling according to mass is performed.

$$S = S_{\mathrm{p}} + S_{\mathrm{np}} = S_{\mathrm{p}} + \frac{\Delta_{\mathrm{np}}}{m} \tag{18.17}$$

$$S_{\mathrm{p}} = (S - \frac{\Delta_{\mathrm{np}}}{m}) \cdot \frac{m_{\mathrm{phantom}}}{m_{\mathrm{true}}} \tag{18.18}$$

$$S_{\mathrm{recalculated}} = (S - \frac{\Delta_{\mathrm{np}}}{m}) \cdot \frac{m_{\mathrm{phantom}}}{m_{\mathrm{true}}} + \frac{\Delta_{\mathrm{np}}}{m} \tag{18.19}$$

The absorbed fractions for photons and electrons vary according to the initial energy and the volume/mass of the target region and, thus, the suitability of the recalculation will also vary, as was discussed in the previous section (Fig. 18.5).

The principle of reciprocity means that the *S* value is approximately the same for a given combination of source and target regions, i.e. $S(r_T \leftarrow r_S)$ is equal to $S(r_S \leftarrow r_T)$. The reciprocity principle is only truly valid under ideal conditions, in regions with a uniformly distributed radionuclide within a material that is either (i) infinite and homogenous or (ii) absorbs the radiation without scatter. The ideal conditions are not present in the human body, although the reciprocity principle can be seen in *S* value tables for human phantoms as the numbers are almost mirrored along the diagonal axis of the table.

S values for a sphere of a certain volume and material should be scaled according to density if the material in the sphere is different from the material in the phantom (Eq. (18.20)). The technique can be applied when an *S* value for a unit density sphere is used for the calculation of the absorbed dose to a tumour made up of bone or lung. However, it should be noted that an *S* value with the correct mass could be chosen instead of scaling the *S* value for the correct volume by the density.

$$S_{\text{volume, material X}} = S_{\text{volume, material Y}} \cdot \frac{\phi_{\text{material Y}}}{\phi_{\text{material X}}} \tag{18.20}$$

18.1.4. Strengths and limitations inherent in the formalism

Two assumptions are automatically made when the MIRD formalism is applied:

(a) The activity distribution in the source region is assumed to be uniform;
(b) The mean absorbed dose to the target region is calculated.

These assumptions are approximations of the reality. The strengths of the MIRD implementation are its simplicity and ease of use. The limitation of these assumptions is that the absorbed dose may vary throughout the region.

It is important to note that the MIRD formalism does not set any restrictions on either the volume or the shape of the source or target, as long as uniformity can be assumed. This means that the source and target volumes could be defined so that the condition of uniformity is met.

The absorbed dose *D* is defined by the International Commission on Radiation Units and Measurements as the quotient of the mean energy imparted $\mathrm{d}\bar{\varepsilon}$ and the mass d*m* [18.8]:

$$D = \frac{\mathrm{d}\bar{\varepsilon}}{\mathrm{d}m} \tag{18.21}$$

The absorbed dose is defined at a point, but it is determined from the mean specific energy and is, thus, a mean value. This is more obvious from an older definition of absorbed dose, where it is defined as the limit of the mean specific energy as the mass approaches zero [18.9]:

$$D = \lim_{m \to 0} \bar{z} \tag{18.22}$$

The dosimetric quantity that considers stochastic effects and is, thus, not based on mean values, is the specific energy z. The specific energy represents a stochastic distribution of individual energy deposition events ε divided by the mass m in which the energy was deposited [18.10]:

$$z = \frac{\varepsilon}{m} \tag{18.23}$$

The unit of the specific energy is joules per kilogram and its special name is gray. Its relevance is especially important in microdosimetry which is the study of energy deposition spectra within small volumes corresponding to the size of a cell or cell nucleus.

The energy imparted to a given volume is the sum of all energy deposits ε_i in the volume:

$$\varepsilon = \sum_i \varepsilon_i \tag{18.24}$$

The energy deposit is the fundamental quantity that can be used for the definition of all other dosimetric quantities. Each energy deposit is the energy deposited in a single interaction i:

$$\varepsilon_i = \varepsilon_{\text{in}} - \varepsilon_{\text{out}} + Q \tag{18.25}$$

where

ε_{in} is the kinetic energy of the incident ionizing particle;
ε_{out} is the sum of the kinetic energies of all ionizing particles leaving the interaction;

and Q is the change in the rest energies of the nucleus and of all of the particles involved in the interaction.

If the rest energy decreases, Q has a positive value and if the rest energy increases, it has a negative value. The unit of energy imparted and energy deposited is joules or electronvolts. The summation of the energy deposits to receive the energy imparted may be performed for one or more events, which is a term denoting the energy imparted from statistically correlated particles, such as a proton and its secondary electrons.

The absorbed dose is a macroscopic entity that corresponds to the mean value of the specific energy per unit mass, but is defined at a point in space.

When considering an extended volume such as an organ in the body, then for the mean absorbed dose to be a true representation of the absorbed dose to the target volume, either radiation equilibrium or charged particle equilibrium must exist. Radiation equilibrium means that the energy entering the volume must equal the energy leaving the volume for both charged and uncharged radiation. The conditions under which radiation equilibrium are present in a volume containing a distributed radioactive source are [18.11]:

— The radioactive source must be uniformly distributed;
— The atomic composition of the medium must be homogeneous;
— The density of the medium must be homogeneous;
— No electric or magnetic fields may disturb the paths of the charged particle.

Charged particle equilibrium always exists if radiation equilibrium exists. However, charged particle equilibrium can exist even if the conditions for radiation equilibrium are not fulfilled.

If only charged particles are emitted from the radioactive source (as is the case for β emitters such as ^{90}Y and ^{32}P), charged particle equilibrium exists if radiative losses are negligible. Radiative losses increase with increasing electron energy and with an increase in the atomic number of the medium. The maximum β energy for pure β emitters commonly used in nuclear medicine (e.g. ^{90}Y, ^{32}P and ^{89}Sr) is less than 2.5 MeV and the ratio of the radiative stopping power to the total stopping power is 0.018 and 0.028 for skeletal muscle and cortical bone, respectively, for an electron energy of 2.5 MeV. This would imply that the radiative losses can be neglected in internal dosimetry and charged particle equilibrium can be assumed.

If both charged and uncharged particles (photons) are emitted (as is the case with most radionuclides used in nuclear medicine), charged particle equilibrium exists if the interaction of the uncharged particles within the volume is negligible. A negligible number of interactions means that the photon absorbed fraction is low. Photon absorbed fractions as a function of mass can be seen in Fig. 18.5, but it should be pointed out that the relative photon contribution for a radionuclide is also dependent on the energy and the probability of emission of electrons. For example, the photon contribution to the absorbed dose cannot be disregarded for ^{111}In in a 10 g sphere, where the photons contribute 45% to the total *S* value.

18.1.4.1. Non-uniform activity distribution

The activity distribution is seldom completely uniform over the whole tissue. This effect was theoretically investigated on a macroscopic level by Howell et al. [18.12] by introducing activity distributions that varied as a

function of the radius of a sphere. The non-uniformity in the activity distribution can be overcome by redefining the source region into a smaller volume. This is a feasible approach until the activity per unit volume becomes small enough to cause a break-down of both radiation and charged particle equilibrium.

Redistribution of the radioactive atoms over time is responsible for creating non-uniformities of the absorbed dose distribution over time. This effect is handled indirectly in the MIRD formalism, which utilizes the concept of cumulated activity, defined as the total number of decays during the time of integration. However, in most practical applications of MIRD dosimetry, heterogeneities of source distribution within organs are neglected.

18.1.4.2. Non-uniform absorbed dose distribution

If the activity of an α or β emitting radionuclide is uniformly distributed within a sphere, then the absorbed dose distribution will be uniform from the centre of the sphere out to a distance from the rim corresponding to the range of the most energetic particle emission. If the radius of the sphere is large relative to the particle emission ranges, then radiation equilibrium will be established except at the rim and the mean absorbed dose will give a representative value of the absorbed dose. If the radius of the sphere is of the same order as the range of the emitted electrons, significant gradients in the absorbed dose distribution will be formed at the borders of the sphere. As a rule of thumb, it can be assumed that the absorbed dose at the border of the sphere will be half of the absorbed dose at the centre. If the sphere is small compared to the range of the electrons, charged particle equilibrium is never established and the absorbed dose distribution will never be uniform inside the sphere. For α emitting radionuclides, the absorbed dose is uniform for almost all sized spheres, except within 70–90 μm from the rim, corresponding to the α particle range.

Interfaces between media, such as soft tissue/bone or soft tissue/air, will cause non-uniformity in the absorbed dose distribution due to differences in backscatter. This can be significant when estimating the contribution of absorbed dose to the stem cells in the bone marrow from backscatter off the bone surfaces. For planar geometry, the maximum increase in absorbed dose was 9%, as determined by Monte Carlo simulations of ^{90}Y. Experimental measurements with ^{32}P showed a maximal increase of 7%, in close agreement with the theoretical estimates. For a spherical interface with a 0.5 mm radius of curvature, the absorbed dose to the whole sphere showed a maximum increase for 0.5 MeV electrons of as much as 12%.

Non-uniformities in the absorbed dose distribution will also be caused by the cross-absorbed dose, i.e. when one organ is next to another such as lung and heart. In human subjects, the separation between organs is sufficiently great

that the cross-absorbed dose results from penetrating photon radiation only. It is important to note that the cross-organ absorbed dose from high energy β emitters, such as ^{90}Y and ^{32}P, can be significant in preclinical small animal studies used to study radiation toxicity. The importance of the cross-absorbed dose in comparison to the self-absorbed dose strongly depends on both the *S* value and the relative size of the time-integrated activity within the source and the target regions.

The MIRD formalism as such is equally applicable to any well defined source and target region combinations [18.13, 18.14]. Depending on the volume and dimensions of the regions, different types of emitted radiation will be of different importance. To conclude the above discussion, a number of factors causing non-uniformity in the absorbed dose distribution have been identified:

— Edge effects due to lack of radiation equilibrium;
— Lack of radiation equilibrium and charged particle equilibrium in the whole volume (high energy electrons emitted in a small volume);
— Few atoms in the volume, causing a lack of radiation equilibrium and introduction of stochastic effects;
— Temporal non-uniformity due to the kinetics of the radiopharmaceutical;
— Gradients due to hot spots;
— Interfaces between media causing backscatter;
— Spatial non-uniformity in the activity distribution.

18.2. INTERNAL DOSIMETRY IN CLINICAL PRACTICE

18.2.1. Introduction

Internal dosimetry is performed with different purposes, which would require different levels of accuracy in the calculated absorbed dose, depending on the subgroup:

— Dosimetry for diagnostic procedures utilized in nuclear medicine;
— Dosimetry for therapeutic procedures (radionuclide therapy);
— Dosimetry in conjunction with accidental intake of radionuclides.

The dosimetry for a diagnostic procedure is performed to optimize the procedure concerning radiation protection consistent with the requirements of an accurate diagnostic test. This is an optimization of a clinical procedure applicable to all persons. The most relevant would, therefore, be to utilize the mean pharmacokinetics for the radiopharmaceutical for the calculation of the time-integrated activity and *S* values based on a reference man

phantom. The ICRP has published the absorbed dose per injected activity for most radiopharmaceuticals used for diagnostic procedures in the clinic in Publication 53 [18.5], with updates published in Publications 80 and 106 [18.15, 18.16].

The purpose of performing dosimetry for a patient that receives radionuclide therapy is to optimize the treatment so as to achieve the highest possible absorbed dose to the tumour, consistent with absorbed dose limiting toxicities. Thus, individualized treatment planning should be performed that takes into account the patient specific pharmacokinetics and biodistribution of the therapeutic agent.

The procedure to apply after an accidental intake of radionuclides must be decided on a case by case basis. The procedure to apply will depend on the level of activity, which radionuclide, the number of persons involved, whether the dosimetry is performed retrospectively or as a precaution, and whether there is a possibility to perform measurements after the intake.

18.2.2. Dosimetry on an organ level

Dosimetry on an organ level could be performed from activity quantification using either 2-D or 3-D images. Two dimensional images may include whole body scans or spot views covering the regions of interest. Three dimensional single photon emission computed tomography (SPECT) is mostly a limited field of view study that includes only the essential structures of interest. The advantage of 3-D tomographic methods is that they avoid the problems associated with corrections for activity in overlying and underlying tissues (e.g. muscle, gut and bone), and corrections for activity in partly overlapping tissues (e.g. liver and right kidney). Three dimensional positron emission tomography (PET) is emerging as a powerful dosimetric tool because of the greater ease and accuracy of radiotracer quantification with this modality.

S value tables for human phantoms can be found in MIRD Pamphlet No. 11 [18.17], in the OLINDA EXM software [18.18] and on the RADAR web site (www.doseinfo-radar.com). OLINDA/EXM stands for organ level internal dose assessment/exponential modelling, and is a software for the calculation of absorbed dose to different organs in the body. OLINDA includes *S* values for most radionuclides and for ten different human phantoms (adult and children at different ages as well as pregnant and non-pregnant female phantoms). Tumours are not included in the phantoms, although the *S* values for unit density spheres provided in the software could be applied for the calculation of the self-absorbed dose to the tumour. OLINDA also includes a module for biokinetic analysis, allowing the user to fit an exponential equation to the data entered on the activity in an organ at different time points. *S* values can be scaled by mass within

OLINDA, thus allowing for a more patient specific dosimetry to be performed. MIRDOSE [18.19] is the predecessor of OLINDA/EXM.

When calculating the absorbed dose with the MIRD formalism and using tabulated *S* values for a phantom, for example, the reference man, it is assumed that the patient's anatomy is the same as that of the phantom. To employ the MIRD scheme and yet make the dosimetry more patient specific, the *S* values can be scaled to the mass of each patient's target organ. Owing to the inverse relation between the absorbed dose and the mass of the target region, scaling can have a considerable influence on the result. The organ mass can be estimated from CT, magnetic resonance imaging or ultrasound images, provided that the anatomical size equals the functional size (the volume/mass of the organ that is actually physiologically functioning and has an activity uptake).

$$S_{\text{patient}} \approx S_{\text{phantom}} \cdot \frac{m_{\text{phantom}}}{m_{\text{patient}}} \tag{18.26}$$

Since it requires a great deal of work to determine the mass of every organ for each patient, it was suggested that the *S* values might be scaled to the total mass of the patient. This is a more crude method, assuming that the organ size follows the total mass of the body. The lean body weight of the patient should be used to avoid unrealistic values of the organ mass and, thus, the *S* values due to obese or very lean patients.

$$S_{\text{patient}} \approx S_{\text{phantom}} \cdot \frac{m_{\text{TB,phantom}}}{m_{\text{TB,patient}}} \tag{18.27}$$

Tumours are not included in reference man phantoms. However, *S* values could be used for spheres of the correct mass to get an approximation of the self-absorbed dose to the tumour. The drawback with this method is that neither the contribution from the cross-absorbed dose from activity in normal organs to the tumour nor the cross-absorbed dose from activity in the tumour to normal organs can be included in the calculations.

18.2.3. Dosimetry on a voxel level

The activity in an image could be quantified on a voxel level, to display the activity present in each voxel. Images that display the activity distribution at different points in time after injection may be co-registered to each other to allow for an exponential fit on a voxel by voxel basis. A parametric image that gives the time-integrated activity (the total number of decays) on a voxel level

can, thus, be calculated. Parametric images that display the biological half-life for each voxel could also be produced by this technique.

The registration of the images acquired at different points in time after the administration becomes essential for the accuracy that can be achieved in the calculation of the time-integrated activity on a voxel level. Another important factor that determines the accuracy in the time-integrated activity and, thus, in the absorbed dose, is the acquired number of counts per voxel (a random error), the accuracy in the attenuation correction (systematic error) and the calibration factor that translates the number of counts to the activity (random and systematic errors). Multimodality imaging such as SPECT/CT and PET/CT facilitates the interpretation of the images as the CT will provide anatomical landmarks to support the functional images, which could change from one acquisition to the next.

A dose point kernel describes the deposited energy as a function of distance from the site of emission of the radiation. Figure 18.7 displays a dose point kernel for 1 MeV mono-energetic electrons. Convolution of a dose point kernel and the activity distribution from an image acquired at a certain time after the injection gives the absorbed dose rate. Dose point kernels provide a tool for fast calculation of the absorbed dose on a voxel level. However, the main drawback is that a dose point kernel is only valid in a homogenous medium, where it is commonly assumed that the body is uniformly unit density soft tissue.

Monte Carlo simulations that use the activity distribution from a functional image (PET or SPECT) and the density distribution from a CT image avoid the problem of non-uniform media, although full Monte Carlo simulations are time consuming. EGS (electron gamma shower), MCNP (Monte Carlo N-particle transport code), Geant and Penelope are commonly used Monte Carlo codes.

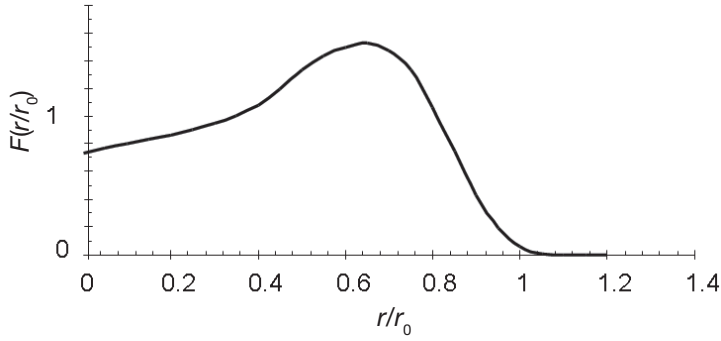

FIG. 18.7. A scaled dose point kernel for 1 MeV electrons [18.20]. r/r_0 expresses the distance scaled to the continuous slowing down approximation range of the electron and $\int_0^\infty F(r/r_0, E_0)\,\mathrm{d}(r/r_0) = 1.$

The concept of dose–volume histograms (DVHs), extensively used to describe the tumour and organ dose distribution in external beam radiotherapy, can be used to display the non-uniformity in the absorbed dose distribution from radionuclide procedures. A differential DVH shows the fraction of the volume that has received a certain absorbed dose as a function of the absorbed dose, while a cumulative DVH shows the fraction of the volume that has received an absorbed dose less than the figure given on the x axis. A truly uniform absorbed dose distribution would produce a differential DVH that shows a single sharp (δ function) peak and a step function on a cumulative DVH. Since the mean absorbed dose in internal dosimetry may be a poor representation of the absorbed dose to the tissue, as discussed above, the use of DVHs might be used to assist the correlation between absorbed dose and biological effect.

REFERENCES

[18.1] STELSON, A.T., WATSON, E.E., CLOUTIER, R.J., A history of medical internal dosimetry, Health Phys. **69** (1995) 766–782.

[18.2] LOEVINGER, R., BERMAN, R.M., A schema for absorbed-dose calculations for biologically-distributed radionuclides, MIRD Pamphlet No. 1, J. Nucl. Med. **9** Suppl. 1 (1968) 7–14.

[18.3] LOEVINGER, R., BUDINGER, T.F., WATSON, E.E., MIRD Primer for Absorbed Dose Calculations (Revised Edition), The Society of Nuclear Medicine, MIRD, Reston, VA (1991).

[18.4] BOLCH, W.E., ECKERMAN, E.F., SGOUROS, G., THOMAS, S.R., A generalized schema for radiopharmaceutical dosimetry — standardization of nomenclature, MIRD Pamphlet No. 21, J. Nucl. Med. **50** (2009) 477–484.

[18.5] INTERNATIONAL COMMISSION ON RADIOLOGICAL PROTECTION, Radiation Dose to Patients from Radiopharmaceuticals, Publication 53, Pergamon Press, Oxford (1987).

[18.6] SEGARS, W.P., TSUI, B.M., FREY, E.C., JOHNSON, G.A., BERR, S.S., Development of a 4-D digital mouse phantom for molecular imaging research, Mol. Imaging Biol. **6** (2004) 149–159.

[18.7] STABIN, M.G., KONIJNENBERG, M.W., Re-evaluation of absorbed fractions for photons and electrons in spheres of various sizes, J. Nucl. Med. **41** (2000) 149–160.

[18.8] INTERNATIONAL COMMISSION ON RADIATION UNITS AND MEASUREMENTS, Fundamental Quantities and Units for Ionizing Radiation, Rep. 60, ICRU, Bethesda, MD (1998).

[18.9] INTERNATIONAL COMMISSION ON RADIATION UNITS AND MEASUREMENTS, Radiation Quantities and Units, Rep. 33, ICRU, Bethesda, MD (1983).

[18.10] INTERNATIONAL COMMISSION ON RADIATION UNITS AND MEASUREMENTS, Microdosimetry, Rep. 36, ICRU, Bethesda, MD (1983).

[18.11] ATTIX, F.H., Introduction to Radiological Physics and Radiation Dosimetry, John Wiley & Sons, New York (1986).

[18.12] HOWELL, R.W., RAO, D.V., SASTRY, K.S.R., Macroscopic dosimetry for radioimmunotherapy: Nonuniform activity distributions in solid tumours, Med. Phys. **16** (1989) 66–74.

[18.13] HOWELL, R.W., The MIRD schema: From organ to cellular dimensions, J. Nucl. Med. **35** (1994) 531–533.

[18.14] KASSIS, I.E., The MIRD approach: Remembering the limitations, J. Nucl. Med. **33** (1992) 781–782.

[18.15] INTERNATIONAL COMMISSION ON RADIOLOGICAL PROTECTION, Radiation Dose to Patients from Radiopharmaceuticals (Addendum to ICRP Publication 53), Publication 80, Pergamon Press, Oxford and New York (1998).

[18.16] INTERNATIONAL COMMISSION ON RADIOLOGICAL PROTECTION, Radiation Dose to Patients from Radiopharmaceuticals (Addendum 3 to ICRP Publication 53), Publication 106, Elsevier (2008).

[18.17] SNYDER, W.S., FORD, M.R., WARNER, G.G., WATSON, S.B., MIRD Pamphlet No. 11, S, Absorbed Dose per Unit Cumulated Activity for Selected Radionuclides and Organs, The Society of Nuclear Medicine, Reston, VA (1975).

[18.18] STABIN, M.G., SPARKS, R.B., CROWE, E., OLINDA/EXM: The second-generation personal computer software for internal dose assessment in nuclear medicine, J. Nucl. Med. **46** (2005) 1023–1027.

[18.19] STABIN, M.G., MIRDOSE: Personal computer software for internal dose assessment in nuclear medicine, J. Nucl. Med. **37** (1996) 538–546.

[18.20] BERGER, M., Improved point kernels for electron and beta-ray dosimetry, NBSIR 73–107, National Bureau of Standards (1973).